




Thermoplastic polyurethane/butylene-styrene triblock copolymer blends: an alternative to tune wear behavior

Lucas Dall Agnol¹ · Giulio Tremea Toso² · Fernanda Trindade Gonzalez Dias³ · Márcio Ronaldo Farias Soares^{1,4} · Otávio Bianchi^{1,2,4} 

Received: 22 February 2021 / Revised: 16 April 2021 / Accepted: 22 May 2021

© The Author(s), under exclusive licence to Springer-Verlag GmbH Germany, part of Springer Nature 2021

Abstract

This work presents an interesting alternative for improving thermoplastic polyurethane's (TPUs) tribological properties by incorporating styrene-ethylene/butylene-styrene triblock copolymer (SEBS) via melt blending. Two TPUs with different molar masses, two compatibilizers SEBS-*g*-MA (C1) and SEBS-*b*-TPU (C2) and paraffinic oil were used in the formulated blends. The raw materials' effect on the morphology, rheology, physical–mechanical and tribological performance of TPU/SEBS blends was monitored. The phase morphology achieved depended on the addition of mineral oil and compatibilizer agent type. The rheological analysis showed a pseudo-liquid viscous behavior for all samples. However, this behavior was related to the compatibilizer type and molar mass of the TPU. No significant changes were observed between the compatibilizers C1 and C2 concerning the physicomechanical properties. The fact that mineral oil is preferentially contained in the SEBS phase is the fundamental point to explain the blends phase morphology and their rheological and physical behaviors. The swollen state SEBS modifies the TPU's performance. It also allows tuning properties such as abrasion and increasing the friction coefficient, enabling promising applications for these thermoplastic elastomers blends.

Keywords Thermoplastic polyurethane · Polymer blends · Compatibilization · SEBS · Tribological properties

✉ Otávio Bianchi
otavio.bianchi@gmail.com

- ¹ Postgraduate Program in Materials Science and Engineering (PGMAT), University of Caxias do Sul, Caxias do Sul, RS, Brazil
- ² Postgraduate Program in Mining, Metallurgical and Materials Engineering (PPGE3M), Federal University of Rio Grande do Sul (UFRGS), Porto Alegre, RS, Brazil
- ³ Postgraduate Program in Technology and Materials Engineering (PPG-TEM), Federal Institute of Education, Science and Technology of Rio Grande do Sul (IFRS), Campus Feliz, RS, Brazil
- ⁴ Department of Materials Engineering (DEMAT), Federal University of Rio Grande do Sul (UFRGS), Porto Alegre, RS, Brazil

Introduction

Thermoplastic polyurethanes (TPU) play an increasingly important role in the polymer industry. Their wide spectrum of properties like tensile strength, resilience, resistance to solvents and chemicals, besides high versatility in chemical structures and ease of processing, enable them to be used in many applications [1–3]. These compounds are block copolymers constituted by hard and soft segments. As a result of thermodynamic incompatibility between the segments, these materials experience microphase segregation [4]. The flexible phase is a polyol that offers the rubber-like characteristics and elasticity of the elastomers. The diisocyanate reaction produces the rigid phase and short-chain diols employed as chain extender affects the mechanical features, like elasticity, hardness and tearing strength [2, 4]. By varying the amount of hard and soft phases, the properties of the TPU can be tunable easily to their respective applications. Among tribological applications, for example, these materials are used as high-performance shoe soles, transport belts, tires, rollers and bushings, etc. [5, 6]. Moreover, the structure of TPU is predisposed to damage throughout a most rigorous friction effort, generating a significant mass loss in the material during application. Thus, the performance of TPU still requires to be further enhanced. Various methods have been suggested to augment the wear resistance of TPU, for example, the selection of particular polyols, highly wear-resistant and self-lubricating fillers. Another simpler alternative that has been of considerable interest in recent years is the blending of TPU with other polymers [1, 6, 7].

Styrene-ethylene/butylene-styrene triblock copolymers (SEBS) are polymers frequently used to blend with TPU due to their potential applications in the consumer and automotive industry, insulation and cable sheathing [2, 8–11]. The main aim has been to reduce cost, improve thermal stability and promote blend compatibility. SEBS is formed from the hydrogenation of the butadiene block present in the styrene butadiene styrene (SBS) copolymer [12]. Similar to TPU, the SEBS microstructure has phase separation. The styrene phase is responsible for the rigid phase at the copolymer and poly(ethylene butylene) ends for the flexible phase at the center of the molecule [9, 13–15]. The blends of TPU and SEBS can result in suitable wear resistance materials, thus significantly improving the system's tribological performance [16]. While the TPU's aromatic rigid blocks seem to associate with the SEBS network, especially with the polystyrene segment's phenyl side-groups, the aliphatic polyether soft segments of TPU can interact with the ethylene/butylene block of SEBS [10]. In general, the weak-phase separation between the constituents always ends up being noticed. However, the polymer blends system enhanced by hydrogen-bonding interactions can result in higher energy dissipation during the friction process [16].

Nevertheless, an intrinsic limitation of TPU/SEBS blending preparation is its compatibility due to the van der Waals interaction being low energy magnitude [2]. The use of suitable block or graft copolymers as compatibilizers for such immiscible polymer blends is necessary to improve the blends' compatibility and properties. Typically, these grafted or block copolymers have structural segments

in which the segments can interact with a polymer or another segment, reducing the polymer's immiscibility. The literature has shown that the use of compatibilizers such as styrene–ethylene–butylene styrene grafted with maleic anhydride (SEBS-g-MA) [2, 8, 17], maleic anhydride grafted ethylene-propylene rubber (EPM-g-MA) [2] and polyurethane blocked styrene–ethylene–butylene–styrene (SEBS-b-TPU) [18] is interesting strategy in the compatibility of SEBS blends with TPU, polyamide 6, polyphenylene, etc. In general, there is a reduction in the phase domains and an improvement in the mechanical properties.

Naskar et al. [2, 8, 17] showed that dramatic changes from a nonuniform to finer and uniform dispersed phase morphology occur with the addition of compatibilizers (SEBS-g-MA and EPM-g-MA) in SEBS/TPU blends. Also, chemical changes in the blends brought about by the interactions between blend components and compatibilizers were observed. This was reflected in higher thermal resistance, higher tensile strength and elongation at break for the entire compatibilized blends. Melt rheological analysis showed a molecular build-up in the system and directly correlated to the mixing pattern of the blends. Wu et al. [9] reported that the thermal stability, dynamic damping characteristics and mechanical performance of SBS/TPU blends are improved as the incorporated TPU increases. Bolados et al. [10] analyzed TPU's effect on a thermoplastic dielectric elastomer's actuation response, such as SEBS. The addition of 10 wt.% of TPU to SEBS significantly increased actuation strain without negatively altering the dielectric breakdown strength. Lu et al. [11, 18] produced high-performance SEBS/TPU blends containing SEBS-b-TPU and SEBS-b-TPU/clay or organo-modified montmorillonites by melt mixing and obtained an improvement in the thermal stability. There was also an enhancement in mechanical and rheological characteristics, as supposed. Meanwhile, the abrasion resistance of SEBS/TPU blends was considerably improved by the presence of SEBS-b-TPU/clay. The DIN volume loss decreased by as much as 56%, which can be explained by nanoscale dispersion of the clay platelets improved the ability of the TPUs to resist fracture or tearing, as well as the increased interfacial adhesion between SEBS and TPU.

Except for the properties mentioned above, as far as we know, there are no studies on the wear characteristics of these mixtures, mainly when SEBS is used in thermoplastic elastomer blend to improve TPU properties. We are interested in obtaining TPU/SEBS blends using a twin co-rotating twin-screw extruder in this context. Two TPUs with different molar masses, two compatibilizers (SEBS-g-MA and SEBS-b-TPU) and paraffinic oil were selected to evaluate the morphology, rheology and physical–mechanical performance of SEBS/TPU blends. We also intend to assess the blend's tribological properties with the potential application of this material as utensil cables, sporting goods, footwear and other devices that require a specific coefficient of friction.

Materials and methods

Materials

Two thermoplastic polyurethanes (T1, with a viscosity of 1200 cps and molecular weight of 92,027 g/mol and T2, with a viscosity of 140 cps and molecular weight

of 57,104 g/mol), both composed of 4,4'-diphenylmethane diisocyanate (MDI) hard segment and polyester-based soft segment, were provided by FCC Ltda (Brazil). The polymers' viscosity was measured from a 15 wt.% solution in dimethylformamide and the molecular weight was measured by gel permeation chromatography (GPC, Viscotek TDAmix) in THF (1 m/min at 45 °C using PS standard). SEBS containing 32 wt.% styrene, trade name Taipol-SEBS-3151 (entitled as S1) with a viscosity of 1700 cps (measured from a 10 wt.% solution in toluene) was supplied by TSRC Corporation (China). Two types of compatibilizers were used: SEBS FG-1901 (entitled as C1), a SEBS grafted with maleic anhydride (2%), was supplied by Kraton Polymers do Brasil (Brazil); the second grade used was Septon TU-S5265 (entitled as C2), a block copolymer of the polyester TPU and SEBS, purchased from Kuraray America Inc. (USA). Paraffinic oil (Paralux 6001) with a viscosity of 100 SUS at 40 °C was purchased from Chevron Renkert (USA). Irganox 1010 primary antioxidant and Irgafos 168 secondary antioxidant were supplied by BASF S.A. (China). All solvents were analytical grade, and all other chemicals were used as received. Before processing, TPU and SEBS were dried in an oven for 24 h at 80 °C.

Blend preparation

The blends were melt processed in an interpenetrating co-rotating twin-screw extruder with a 40 L/D and 25 mm diameter (D) (ICMA San Giorgio). The composition of the blends is summarized in Table 1. In all samples, 15 wt.% paraffinic oil was added to facilitate processing due to the styrene thermoplastic elastomers' high viscosity. Besides, 0.1 wt.% antioxidants Irganox 1010 and Irgafos 168 were added to prevent the polymer's degradation during extrusion. The extrusion was conducted with a 400 rpm screw speed and a 150–210 °C temperature profile. The feeding rate was maintained at approximately 5 kg/h. The screw profile used for extrusion has three mixing zones interspersed by transport zones, the final and initial transport zones only.

After extrusion, the pelletized blends were dried for 4 h at 80 °C and injection molded (HIMACO injector, injection pressure=9.8 MPa, time 6 s.) to form tensile and impact specimens using 3- and 6-mm-thick plates. The barrel

Table 1 Composition of the TPU/SEBS blends prepared (in wt.%)

Sample code	TPU (T1)	TPU (T2)	SEBS (S1)	Compatibility Agent (C1)	Compatibility Agent (C2)	Paraffin oil
T1	100	–	–	–	–	–
T1S1	75	–	10	–	–	15
T1S1C1	75	–	5	5	–	15
T1S1C2	75	–	5	–	5	15
T2	–	100	–	–	–	–
T2S1	–	75	10	–	–	15
T2S1C1	–	75	5	5	–	15
T2S1C2	–	75	5	–	5	15

temperature profile was 160 °C (hopper) to 180 °C (nozzle), and the mold temperature was maintained at 80 °C.

Blends morphology

The blends morphology was investigated by field emission gun scanning electron microscopy (FEG-SEM) in a Tescan Mira 3 (Czech Republic) microscope. All samples were cryofractured in liquid nitrogen and immersed in methylcyclohexane for 1 h at 80 °C to extract the SEBS phase and reveal the blends' phase boundaries. The solvent etched samples were dried at 80 °C for 24 h. All samples were sputter-coated with gold before imaging.

The SEBS phase was dissolved in methylcyclohexane ($\delta = 16.42 \text{ MPa}^{1/2}$ [19]), which was selected for its similar solubility to SEBS. The samples were placed in a 120-mesh sieve containing approximately 0.3 g of polymer and washed in a round-bottomed flask containing methylcyclohexane at 80 ± 3 °C for 24 h. After solvent extraction, all samples were dried at 80 °C for 24 h. The reaction degree was determined by the weight difference between the extracted SEBS and the one initially incorporated into the blend.

Mechanical properties

Tensile tests were performed on an EMIC-DL500 universal machine, according to ASTM D412, type C format. Dumbbell specimens with a gauge length of 25 mm and a width of 4 mm were stretched at a crosshead speed of 500 mm/min until rupture. Hardness tests were performed according to ASTM D2240 using a Bareiss Shore A analog hardness tester in a 6-mm-thick plate with a measurement time of 3 s. Abrasion tests were performed according to ISO 4649 on a DIN Maqtest abrasimeter from samples with dimensions of 6 mm thick and 13 mm diameter. The surfaces of the blends were analyzed by SEM (Shimadzu SSX-550) after abrasion tests. During all mechanical tests, the room temperature was maintained at 23 ± 2 °C and relative humidity of $36 \pm 2\%$. Five specimens from each sample were assayed for all tests.

Small-amplitude oscillatory shear measurements (SAOS)

The rheological behavior of the neat TPUs and the blends were analyzed in an Anton Paar MCR 301 rheometer using plate-plate geometry with 1 mm gap. Sample discs (25 mm diameter and 3 mm thickness) were fabricated by injection molding. The analyses were performed on 190 °C in a nitrogen atmosphere at a frequency range of 0.1–500 rad/s and a small strain amplitude of 1% (within the linear viscoelastic regime).

Dynamic mechanical analysis (DMA)

The samples' dynamic mechanical analysis of the samples was measured using a dynamic mechanical analyzer (DMA 2980, TA Instruments) with a single cantilever bending mode. Rectangular samples (17.5 mm×12 mm×2.5 mm) were cut from the injection-molded specimens. The temperature range was from $-100\text{ }^{\circ}\text{C}$ to $150\text{ }^{\circ}\text{C}$ at a heating rate of $2\text{ }^{\circ}\text{C}/\text{min}$ in a nitrogen atmosphere with a constant frequency of 1 Hz and an amplitude of $30\text{ }\mu\text{m}$.

Tribological properties

The friction properties were determined by sled-type experiments, according to ASTM D1894-14, taking into account that wear depends on the operation conditions such as normal load, sliding velocity, running time, temperature, counterpart texture and presence of abrasives [20, 21]. In this test, the sample slides on a set roughness substrate, under a normal load and a load cell registers the tangential force as a function of the sliding distance, enabling the estimation of friction coefficient. A surface of the polished glass was employed as an abrasive substrate. The tests were carried out in dry conditions on square-shaped specimens (side 25 mm and thickness 3 mm), glued on a wooden sample holder, at room temperature with a relative humidity $32\pm 2\%$. The initial normal force applied was 1.203 N and the sliding speed was 300 mm/min (sliding distance was 30 cm). Different normal forces by using friction sleds of different weights were tested. The used friction plate was cleaned with acetone between the individual experiments. Each measuring run was repeated three times.

Results and discussion

Blends phase morphology

The physicommechanical behavior of the polymer blends depends intensely on the shape and size of the dispersed phase. Hence, control of morphology in such blends is crucial [22]. Figure 1 shows the TPU/SEBS blends' micrographs after the SEBS phase is removed from the blends by methylcyclohexane extraction, (a–c) represents the SEM images of T1/SEBS blends while (d–f) are the micrographs of T2/SEBS blends. Before extraction, all micrographs showed a uniform phase morphology, with smooth fractured regions. Nevertheless, it was impossible to identify well-defined interfaces between TPU and SEBS phases (data not shown). After SEBS extraction, the blends containing only TPU/SEBS (Fig. 1a and d) exhibited a nonhomogeneous two-phase morphology with the dispersed phase's coarser size, evidencing the poor interfacial adhesion between the two phases. When the compatibilizer was added (Fig. 1b, c, e and f), the morphology changed from two-phase morphology to a fine droplet morphology in which

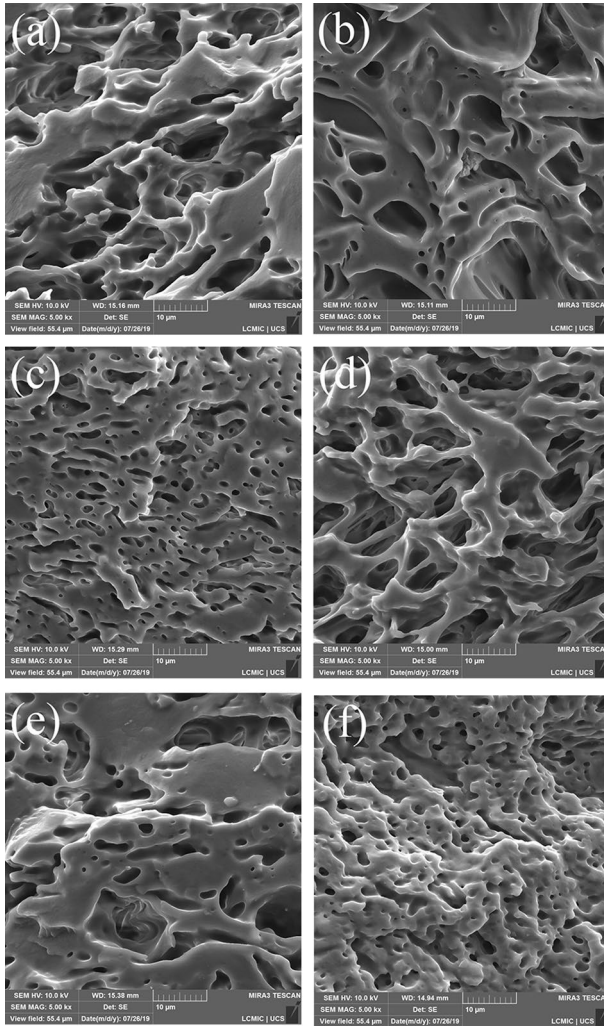


Fig. 1 Phase morphologies after selective etching of TPU/SEBS blends: **a** T1S1, **b** T1S1C1, **c** T1S1C2, **d** T2S1, **e** T2S1C1 and **f** T2S1C2

SEBS is dispersed in the TPU matrix. A similar phase morphology pattern was observed by Anagha e Naskar [8], who attributed it to reactive blending as an efficient method to blends compatibilizer. The added compatibilizer reaches the blend interface by a series of sequences starting from melting, dispersion, solubilization and molecular dispersion. The presence of this graft polymer at the blend interface minimizes the resistance to minor phase destruction during melt mixing; therefore, it prevents the coalescence of particles by forming shells around the droplets and thus results in smaller-sized dispersed domains [2, 8, 23].

Regarding the difference between the morphology presented by the addition of the compatibilizer C2 compared to C1 (Fig. 1b and c), the blends containing C2 showed smaller SEBS domains, with a finer dispersion. Blends containing C1, it is anticipated that the maleic anhydride groups in SEBS-g-MA react with the isocyanate group in TPU and resulting in an imide formation [8, 17, 18]. For C2, it is believed that because it is a copolymer with grafted SEBS groups, the interaction between the phases can be improved due to the grafted segment's size. The difference in SEBS domains' size was smaller for samples with C2, as reported in the literature [18].

Selective extraction in methylcyclohexane solvent was used to quantify the unreacted SEBS content in the materials. Constant amounts of SEBS extracted were observed even for blends with compatibilizer, which indicates that the mineral oil added is mainly contained in the SEBS phase [24]. The values of the quantities extracted in samples T1, T2, T2S1, T2S1C1 and T2S1C2 were 2.9, 4.0, 28.9, 27.4 and 26.1 wt.%, respectively. For neat TPUs, the solvent could extract a small amount that is probably related to low molecular weight molecules. For the blends with SEBS, the value extracted is close to SEBS and oil added initially. When a fine morphology is formed in the blends with compatibilizer, the phase extracted amount was less than the theoretical value. Therefore, based on the similarity of the mass removed from the samples, it is possible to assume that oil is mainly in the SEBS phase. In a typical polymer blend with similar viscosity, a dispersed phase morphology is observed when 5 wt.% is added [21]. It is a behavior observed for SEBS, as mineral oil causes the polymer to swell and increase its free volume. As a result, there is an increase in the phase volume and a co-continuous system is observed [24, 25].

Remembering that styrenic copolymers need to be combined with resins and oils to achieve many applications' desired properties. Materials compatible with elastomeric segments make the product softer, while materials compatible with polystyrene segments give rigidity. Process oils such as paraffinic oils are common additives used to decrease hardness and improve processing [24]. Therefore, the hypothesis that paraffinic oil is mainly contained in the SEBS phase and forming a gel is plausible. This approach can be confirmed based on the solubility parameters of the blend components. For paraffinic oil, the solubility parameter found was $16.50 \text{ MPa}^{1/2}$, polybutadiene block $16.90 \text{ MPa}^{1/2}$, ethylene block of $17.37 \text{ MPa}^{1/2}$ and styrene $22.49 \text{ MPa}^{1/2}$, while for the TPU $24.73 \text{ MPa}^{1/2}$ and the compatibilizer C2 of $29.91 \text{ MPa}^{1/2}$ [26].

Rheology and physicochemical properties

Figure 2a–d shows the storage (G') and loss (G'') moduli vs. angular frequency (ω) curves for the TPU/SEBS with different compatibilizers. At low frequencies, G' and G'' increased when compared with neat TPUs. All samples showed a pseudo-liquid viscous behavior, $G' < G''$ from the 0.1–10 rad/s. The higher increases are noted at 0.1 rad/s for the samples without compatibilizer. It is known that the addition of paraffinic and naphthenic oil causes the formation of gel in the SEBS

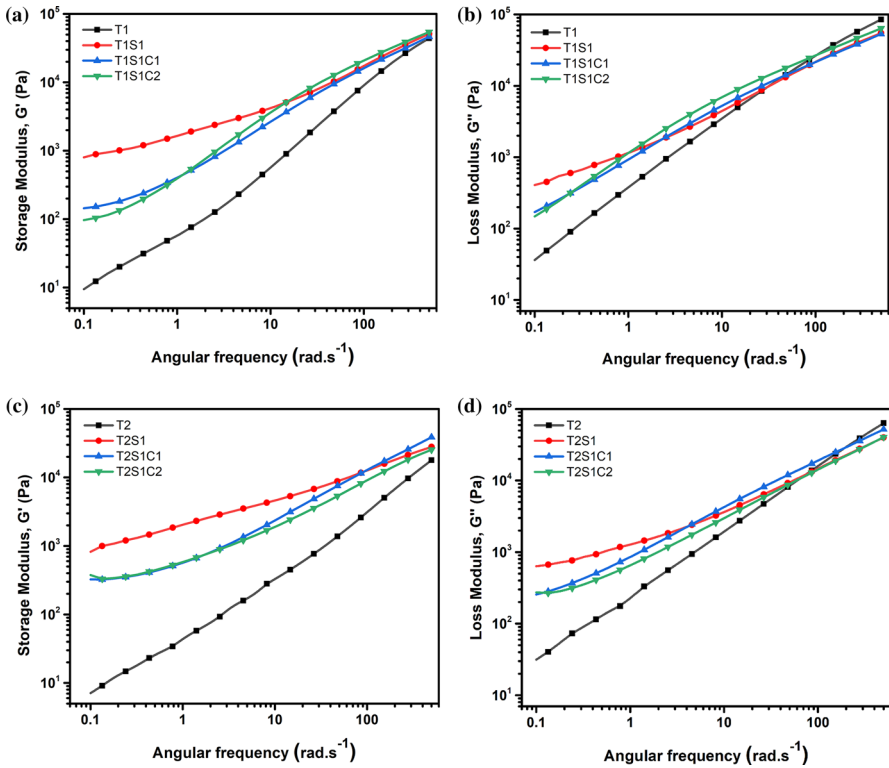


Fig. 2 Logarithmic plots of Loss modulus and Storage modulus as a function of frequency of neat TPU and the blends: **a–b** T1/SEBS system and **c–d** T2/SEBS system

and reduces the ordering temperature and disorder of the blocks (TODT) [24, 25]. The paraffinic/phenolic oil solvates the SEBS chains and increases the free volume. The oil becomes efficient in inducing the macromolecular reptation dynamics' acceleration by allowing the entangled chains to become more widely spaced and provide more reptation volume. Concerning the compatibilized blends, it is believed that the compatibilizer may be limiting the mobility of the swollen phase of SEBS by acting in the interphase boundaries. Thus, both the G' and G'' curves are closer to those of the pure TPU.

The TPUs did not show a crossover point ($G' = G''$) in the analyzed frequencies, while for the T1S1 blend, it was 8 rad/s and T2S1 36 rad/s. The difference found is related to the relaxation time, $\tau_t \sim 1/\omega_{G'=G''}$. Thus, the higher the crossover frequency, the shorter the relaxation time that is directly related to the molar mass values of the polyurethanes ($T1 > T2; \tau_{tT1} > \tau_{tT2}$). On the other hand, when compatibilizers are used, a reduction is noted, mainly due to the oil's low solvency capacity in these molecules (C1 and C2). In this way, they can form more minor phases, as noted in the micrographs of Fig. 1. This effect is due to the polarity of the compatibilizers with the oil, evidenced by the solubility parameters. Because

compatibilizers can be located in the boundary region between the phases, it acts as a barrier and promotes smaller and spherical phases. As a consequence, there is a greater stabilization of the phase morphology.

Differences in viscoelastic response are best appreciated by plotting the phase angle δ as a frequency function, as shown in Fig. 3a and b. Note that $\delta \left[= \text{Tan}^{-1} \left(\frac{G''}{G'} \right) \right]$ measures the viscoelastic response of material: at the limit $\delta \rightarrow 0^\circ$ the response obeys Hook's Law, while $\delta \rightarrow 90^\circ$, the response obeys Newton's Law [27]. T1 shows a slight increase and subsequently, a monotonic reduction of δ after 10 rad/s as the frequency increased from the terminal regime to higher frequencies. A similar trend was seen in T2. Regarding blends, despite the type of TPU, the samples without compatibilizer showed a monotonic increase from the lowest frequencies, leaving a pseudo-elastic behavior for pseudo-liquid, which is related to the formation of a percolated structure in the SEBS phase. In general, blends with compatibilizers act predominantly as energy dissipators; this occurs mainly by forming an interface in the boundary between the TPU and SEBS phases promoted by the compatibilizers.

Figure 4a and b shows the complex viscosity $\left(|\eta^*| = \sqrt{G'^2 + G''^2} / \omega \right)$ as a function of angular frequency. Taking into account that the Cox–Merz relationship $\left(\eta(\dot{\gamma}) \Big|_{\dot{\gamma} \rightarrow 0} = \eta^*(\omega) \Big|_{\omega \rightarrow 0} \right)$ is valid for this system and blends of thermoplastic elastomers. It is possible to notice that the TPU samples show regions with Newtonian plate behavior, while for blends with SEBS, the region with the power fluid behavior was more evident. The shear-thinning behavior as frequency increased only shows increasing free volume and increasing mobility of the SEBS phase. Regarding the viscosity reduction that was noticed in blends with compatibilizer, this effect is attributed to the fact that this agent acts at the interface and contributes to forming a polymer emulsion. Thus the fluid's behavior becomes closer to the TPU. This system has order transitions and block disorder, making formal analysis impossible, as described by Bousmina [28].

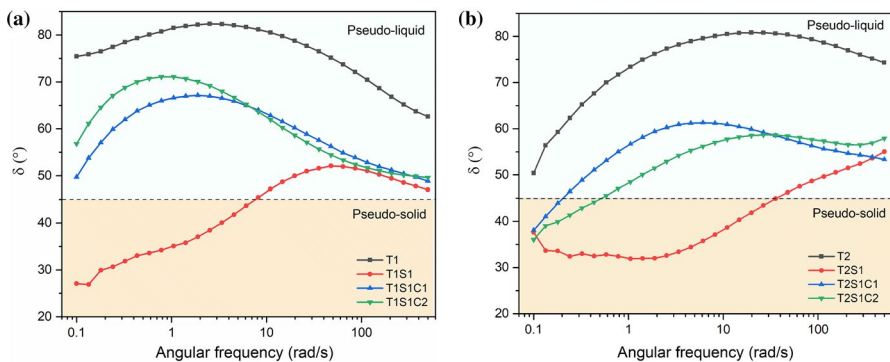


Fig. 3 Phase angle δ as a function of the frequency of oscillation for TPU/SEBS blends

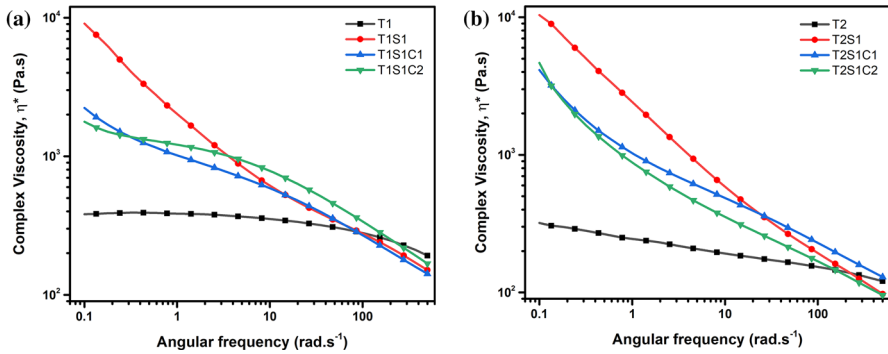


Fig. 4 Logarithmic plots of complex viscosity as a function of frequency of neat TPUs and the blends: **a** T1/SEBS system and **b** T2/SEBS system

Dynamic mechanical analysis (DMA)

DMA provides information regarding the glass transition temperatures that hints at a better understanding of the phase structure and interphase mixing. Figure 5 plots the tan delta at 1 Hz as a function of temperature for neat TPUs and the blends: (a) T1/SEBS system and (b) T2/SEBS system. The storage and loss modules and tan delta δ max are tabulated in Table 2. The neat TPU shows peaks in tan delta around $-9.9\text{ }^{\circ}\text{C}$ for T1 and $-11.4\text{ }^{\circ}\text{C}$ for T2, indicating glass transition temperatures (T_g) in these materials [9]. TPU-T2 also shows a second peak at $76.6\text{ }^{\circ}\text{C}$, relative to the hard segment’s transition. For the blends T1S1 and T2S1, the first peak is found at $-41.1\text{ }^{\circ}\text{C}$, indicating glass transition temperatures of the SEBS. The T_{gs} of elastomeric phases were noted separately for all samples, so it can be inferred that there is no partial miscibility between these phases. However, concerning the transitions of the SEBS and TPU rigid segments, there is an overlap of transitions, making the analysis complex concerning the phases’ miscibility. Thus, separate peaks’ behavior confirms the incompatibility at the microscopic level between the TPU and SEBS

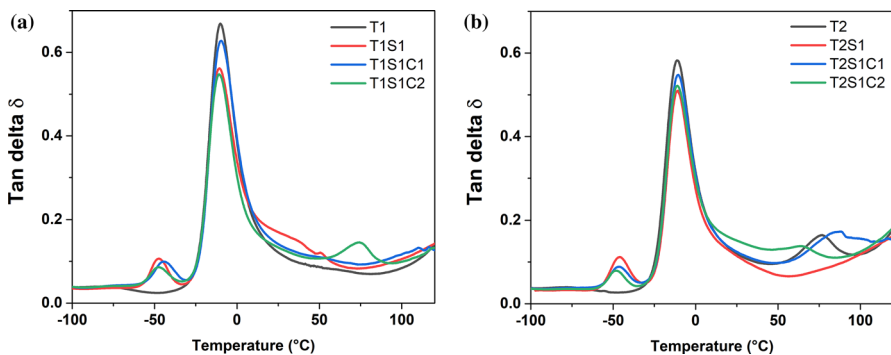


Fig. 5 Tan δ versus temperature plot of pure TPU and the blends: **a** T1/SEBS system and **b** T2/SEBS system

Table 2 Storage modulus, loss modulus and Tan δ values for TPUs and TPU/SEBS blends

Sample code	Storage modulus (MPa)			Loss modulus (MPa)		Tan delta		
	At $-100\text{ }^{\circ}\text{C}$	At $-50\text{ }^{\circ}\text{C}$	At $25\text{ }^{\circ}\text{C}$	Peak 1	Peak 2	Peak 1	Peak 2	Peak 3
T1	4218.3	3273.3	246.5	-78.8	-17.8	-	-9.9	-
T1S1	3291.5	2130.9	148.4	-48.8	-17.8	-47.8	-10.9	-
T1S1C1	2799.2	1845.2	110.3	-46.3	-17.3	-44.8	-9.9	-
T1S1C2	2807.8	1880.9	132.6	-48.8	-17.8	-47.3	-10.4	74.6
T2	4203.3	3405.1	180.3	-73.9	-18.8	-	-11.4	76.6
T2S1	4159.1	2680.3	220.7	-47.8	-17.8	-46.3	-11.4	-
T2S1C1	3105.9	2242.1	142.1	-47.8	-17.8	-46.8	-10.4	87.4
T2S1C2	2956.5	2010.4	172.5	-49.3	-17.8	-46.8	-10.9	64.8

phases [9]. Note that the sample with T1S1C2 showed a peak around $75\text{ }^{\circ}\text{C}$; the same was noticed for T2, which is related to the rigid phase of the TPU [29]. It is worth remembering that SEBS also has a transition from the styrenic phase around $100\text{ }^{\circ}\text{C}$, but due to mineral oil addition, it ends up reducing [9, 30]. Incompatible blends, the first peak changes little for higher temperatures ($-44.8\text{ }^{\circ}\text{C}$ and $-9.9\text{ }^{\circ}\text{C}$). The change may result from interfacial interactions in the blends that occur in the presence of a compatibilizer. A decrease in damping was observed in the blends that possibly the formation *in situ* of a SEBS-g-TPU copolymer. Similar results have also been reported in the literature [17, 18]. Anagha and co-workers [17] showed that the maleic anhydride groups in SEBS-g-MA could react with the isocyanate group in TPU and form the preferred *in situ* graft copolymer SEBS-g-TPU. They showed that the possible group formed by this reaction would be the imide. In general, the presence of a suitable graft polymer at the blend interface prevents particles' coalescence by forming shells around the droplets, resulting in smaller-sized dispersed domains [31]. The stabilization of the morphology with C1 and C2, by both routes of compatibilization, affects the dynamic mechanical properties of the TPU/SEBS blends.

Mechanical properties

Mechanical properties of the TPU/SEBS blends are shown in Table 3. The change observed in morphology was mirrored in their mechanical properties. Sample TPU-T1 showed a tensile strength 44% higher than TPU-T2 (23.9 and 16.7 MPa, for T1 and T2, respectively). However, both showed a similar elongation. It is well known that molar mass substantially influences polymers' tensile properties, especially tensile strength [32, 33]. This can be proven to a higher molar mass and rubbery nature of T1. Based on the premise that the added oil is preferably in the SEBS phase and that there is a reduction in the mechanical properties of this polymer, making the gel fragile [34], TPU/SEBS blends would be expected to show a reduction in the mechanical properties. Thus, the addition of SEBS to the TPU-T1 or TPU-T2 causes

Table 3 Mechanical properties of neat TPUs and TPU/SEBS blends

Samples	Tensile strength (MPa)	Elongation at break (%)	Modulus at 100% elongation (Mpa)	Modulus at 300% elongation (Mpa)	Hardness Shore A
T1	23.9±0.5	708±43	3.9±0.1	7.6±0.2	72±1
T1S1	8.8±0.9	581±48	2.0±0.1	3.9±0.1	54±2
T1S1C1	15.3±0.3	704±26	2.2±0.1	4.6±0.1	60±1
T1S1C2	16.2±0.9	707±29	2.3±0.1	4.7±0.1	59±1
T2	16.7±0.6	675±37	4.6±0.1	8.7±0.2	77±2
T2S1	8.2±0.3	571±22	2.4±0.2	4.7±0.2	59±1
T2S1C1	11.4±0.3	608±18	2.7±0.1	5.6±0.1	63±1
T2S1C2	11.0±0.5	588±15	2.7±0.1	5.7±0.1	62±1

a loss of tensile strength and elongation in the material, a consequence of the weak interfacial adhesion between the polymers with non-uniform phase morphology. The compatibilizers C1 or C2 in the blends caused an improvement in these properties, substantiating the enhancement in interfacial adhesion between TPU and SEBS phases [2, 9]. However, there was no significant difference between the effects of both compatibilizers, according to DMA results.

Regarding the hardness of the material, it is possible to observe that the addition of SEBS in the TPU causes a reduction in this property due to SEBS is in gel form, which results in lower values of hardness modulus. When the compatibilizer is added, the hardness is partially recovered and little difference between the compatibilizers is observed.

Tribological properties

The abrasion resistance was investigated in terms of DIN volume loss. The abrasion and storage modulus values at 25 °C of neat TPUs and blends are shown in Fig. 6. As expected, the TPU-T1 with a higher molar mass and a higher tensile strength shows a higher storage modulus and less abrasive wear volume loss. Previous studies have demonstrated that the effect of abrasion on the TPU initially involves cracks accompanied by the removal of material on the sample surface. Thus, a TPU with higher tensile strength will present greater resistance against cracking/material removal, generating lower DIN abrasion values [32]. The presence of SEBS in the blends caused an increase in the abrasion values related to the phase characteristic at room temperature. SEBS is in gel form, which results in lower values of modulus of elasticity. Thus, small deformations cause deformation and cause it to be pulled out due to the poor interface being weak with the TPU. In all cases, the compatibilizer's addition improved the abrasion wear compared to blends without compatibilizer [18]. The better performance of C2 concerning C1 was also evident. Unlike what happened in the mechanical properties, the finer morphology generated by C2 impacted the abrasion result. A continuous TPU matrix with a greater surface area

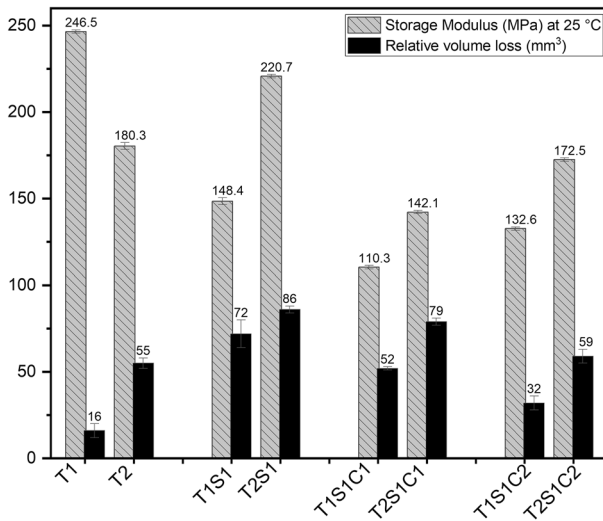


Fig. 6 Storage Modulus at 25 °C and relative volume loss of neat TPUs and TPU/SEBS blends

of contact with the dispersed component will be less susceptible to particle removal due to the wear generated by the abrasimeter.

After the abrasion test, the surfaces of neat TPUs and blends were investigated by SEM and are shown in Fig. 7. All samples evidence a surface damaged with the typical Schallamach's waves, generated by the accumulation of material related to plastic deformation [20, 32]. The parallel wave pattern on the wear surface that perpendicular to the sliding direction is commonly observed for polymers examined by a wear test, resulting from the accumulation of plastic deformation during the reciprocation [32]. Because of the high tensile elongation at break of the model samples, several debris rolls have not been detached during the wear test and are still connected to the wear surface. According to Thomas et al. [35], the fracture patterns formed on the abraded surfaces could be associated to wear resistance, which is related to the particular systems' compatibility, morphology and mechanical properties. The plastic deformation of small fragments within the surface layers proves that the introduction of SEBS contributes little to the system's strength. When it comes to T2S1C2 (Fig. 7h), its abraded surface morphology is the smoothest. The protrusions above the original surface are much smaller than that of other blends, indicating that the introduction of C2 would reduce the distortion and breakage of the composite during the rubbing process.

The knowledge of the polymers' tribological characteristics is essential, mainly concerning the final application. For example, materials with a low friction coefficient can be applied to elastomeric seals for ball-type valves to facilitate the valve's opening and closing. For application as a manual handling tool and safety shoes, materials with higher friction coefficients are normally used to increase the application's security. In this context, the sliding test results are evaluated and calculated by friction coefficients and are shown in Fig. 8. It is seen that the TPU/SEBS

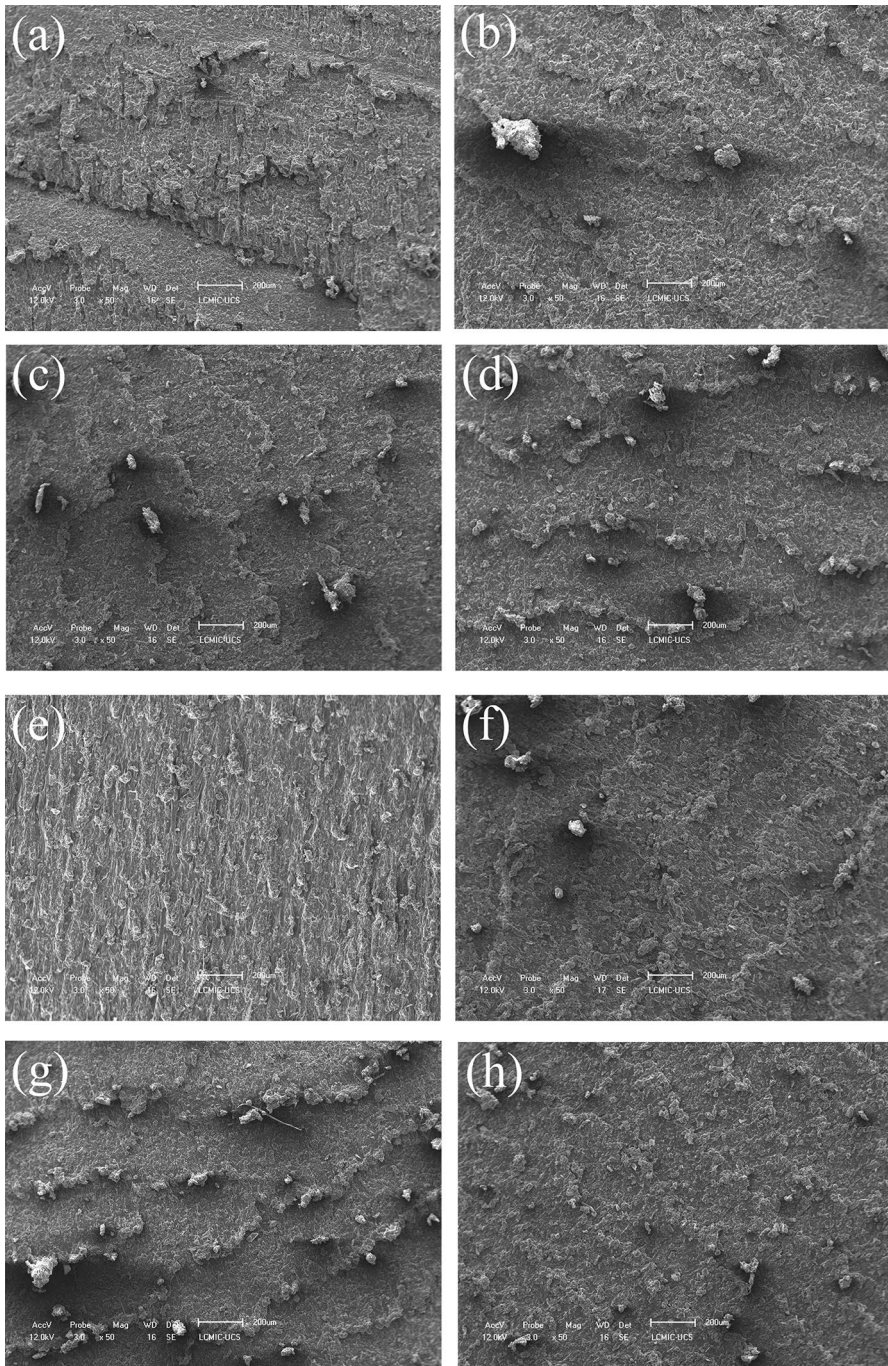


Fig. 7 Abraded surface morphology of pure TPUs and the blends: **a** pure T1, **b** T1S1, **c** T1S1C1, **d** T1S1C2, **e** pure T2, **f** T2S1, **g** T2S1C1 and **h** T2S1C2 (magnification $\times 50$)

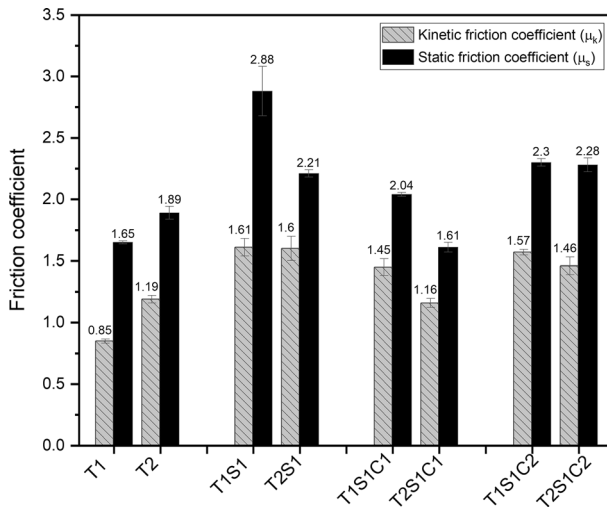


Fig. 8 Static and kinetic friction coefficient values obtained from sled-type experiments

blends have a significantly higher static and kinetic friction coefficient than pure TPU. However, the addition of a compatibilizer caused a reduction in the friction coefficient.

Studies [20, 36] highlight that friction coefficient is dependent on the viscoelastic behavior of the material, being directly proportional to the tangent modulus ($\tan\delta$) and inversely proportional to material hardness. The low values of storage modulus and loss factor demonstrated in the DMA results (Table 2) indicate that the TPU/SEBS material is the softest and most elastic. These data are associated with more significant volume loss during the TPU/SEBS samples' abrasion tests. The higher storage modulus of TPUs can be associated with the higher hardness that results in a lower friction coefficient [37]. The incorporation of SEBS to TPU induces the formation of a gelled structure in the SEBS phase. It has a differential role concerning the friction coefficient, as they make the material processable and an authentic energy sink. The compatibilizers' performance is closely linked to the SEBS phase's distribution in the TPU, which becomes more stable and with less chance of coalescing after reheating for future moldings and obtaining utensils.

Conclusion

In this work, compatibilized TPU/SEBS blends were prepared successfully using a co-rotating twin-screw extruder. The effect of the TPU molar mass, compatibilizer type and the addition of paraffinic oil on the morphological, rheological, physical-mechanical and tribological properties of the blends were investigated. It was evident that mineral oil is mainly in the SEBS phase due to the greater similarity between solubility parameters. Because the SEBS phase is swollen by mineral oil, a fine dispersion in the TPU phase has not always been achieved. Both TPU/SEBS

blends systems with C1 and C2 showed similar mechanical behavior. The fact that SEBS is swollen alters the blend's relaxation dynamics and, consequently, analyzes classic emulsion impossible to apply. The increase in the coefficient of kinetic and static friction promoted by SEBS shows that this blend of thermoplastic elastomers has excellent potential for application in several industrial segments.

Acknowledgements The authors acknowledge financial support from the Brazilian Agency Coordenação de Aperfeiçoamento de Pessoal de Nível Superior (CAPES) for the scholarships to Lucas Dall Agnol and Conselho Nacional de Desenvolvimento Científico e Tecnológico (CNPq, Brazil) for financial support (grant 306086/2018-2). The authors also thank FCC—Indústria e Comércio Ltda for the materials donation.

References

1. Lu Q-W, Macosko CW (2004) Comparing the compatibility of various functionalized polypropylenes with thermoplastic polyurethane (TPU). *Polymer* 45(6):1981–1991. <https://doi.org/10.1016/j.polymer.2003.12.077>
2. Gopalan AM, Naskar K (2019) Ultra-high molecular weight styrenic block copolymer/TPU blends for automotive applications: Influence of various compatibilizers. *Polym Adv Technol* 30(3):608–619. <https://doi.org/10.1002/pat.4497>
3. Agnol LD, Gonzalez Dias FT, Nicoletti NF, Falavigna A, Bianchi O (2018) Polyurethane as a strategy for annulus fibrosus repair and regeneration: a systematic review. *Regen Med* 13(5):611–626. <https://doi.org/10.2217/rme-2018-0003>
4. Hossieny NJ, Barzegari MR, Nofar M, Mahmood SH, Park CB (2014) Crystallization of hard segment domains with the presence of butane for microcellular thermoplastic polyurethane foams. *Polymer* 55(2):651–662. <https://doi.org/10.1016/j.polymer.2013.12.028>
5. Lin C, Tian Q, Chen K, He G, Zhang J, Liu S, Almásy L (2017) Polymer bonded explosives with highly tunable creep resistance based on segmented polyurethane copolymers with different hard segment contents. *Compos Sci Technol* 146:10–19. <https://doi.org/10.1016/j.compscitech.2017.04.008>
6. Li B, Li M, Fan C, Ren M, Wu P, Luo L, Wang X, Liu X (2015) The wear-resistance of composite depending on the interfacial interaction between thermoplastic polyurethane and fluorinated UHMWPE particles with or without oxygen. *Compos Sci Technol* 106:68–75. <https://doi.org/10.1016/j.compscitech.2014.11.005>
7. He T, Wang G, Wang Y, Liu Y, Lai W, Wang X, Feng Y, Liu X (2019) Simultaneously enhancing of wear-resistant and mechanical properties of polyurethane composite based on the selective interaction of fluorinated graphene derivatives. *Compos B Eng* 169:200–208. <https://doi.org/10.1016/j.compositesb.2019.04.014>
8. Anagha MG, Naskar K (2019) Augmentation of performance properties of maleated SEBS/TPU blends through reactive blending. *J Appl Polym Sci* 137(21):48727. <https://doi.org/10.1002/app.48727>
9. Wu J-H, Li C-H, Wu Y-T, Leu M-T, Tsai Y (2010) Thermal resistance and dynamic damping properties of poly (styrene-butadiene-styrene)/thermoplastic polyurethane composites elastomer material. *Compos Sci Technol* 70(8):1258–1264. <https://doi.org/10.1016/j.compscitech.2010.03.014>
10. Aguilar Bolados H, Hernández-Santana M, Romasanta LJ, Yazdani-Pedram M, Quijada R, López-Manchado MA, Verdejo R (2019) Electro-mechanical actuation performance of SEBS/PU blends. *Polymer*. 171:25–33. <https://doi.org/10.1016/j.polymer.2019.03.035>
11. Lu F, Liu Y, Wang F, Yi M, Dy Li (2020) Effect of organo-modified montmorillonite on the morphology and properties of SEBS/TPU nanocomposites. *Polym Eng Sci* 60(4):850–859. <https://doi.org/10.1002/pen.25344>
12. Zhou T, Wu Z, Li Y, Luo J, Chen Z, Xia J, Liang H, Zhang A (2010) Order–order, lattice disordering and order–disorder transition in SEBS studied by two-dimensional correlation infrared spectroscopy. *Polymer* 51(18):4249–4258. <https://doi.org/10.1016/j.polymer.2010.06.051>

13. White CC, Tan KT, Hunston DL, Nguyen T, Benatti DJ, Stanley D, Chin JW (2011) Laboratory accelerated and natural weathering of styrene–ethylene–butylene–styrene (SEBS) block copolymer. *Polym Degrad Stab* 96(6):1104–1110. <https://doi.org/10.1016/j.polyimdegradstab.2011.03.003>
14. Qiao X, Lu X, Gong X, Yang T, Sun K, Chen X (2015) Effect of carbonyl iron concentration and processing conditions on the structure and properties of the thermoplastic magnetorheological elastomer composites based on poly(styrene-*b*-ethylene-co-butylene-*b*-styrene) (SEBS). *Polym Test* 47:51–58. <https://doi.org/10.1016/j.polymertesting.2015.08.004>
15. Wang X, Pang S-l, Yang J-h, Yang F (2006) Structure and properties of SEBS/PP/OMMT nanocomposites. *Trans Nonferrous Met Soc* 16(2):s524–s528. [https://doi.org/10.1016/S1003-6326\(06\)60249-5](https://doi.org/10.1016/S1003-6326(06)60249-5)
16. Jiang S, Yuan C, Guo Z, Bai X (2019) Effect of crosslink on tribological performance of polyurethane bearing material. *Tribol Int* 136:276–284. <https://doi.org/10.1016/j.triboint.2019.03.064>
17. Anagha MG, Chatterjee T, Naskar K (2020) Assessing thermomechanical properties of a reactive maleic anhydride grafted styrene-ethylene-butylene-styrene/thermoplastic polyurethane blend with temperature scanning stress relaxation method. *J Appl Polym Sci* 137(48):49598. <https://doi.org/10.1002/app.49598>
18. Lu F, Liu Y, Gao S, Li D-y, Mai Y-l, Shi H-h, Hu W (2020) SEBS-*b*-TPU and nanoclay: effective compatibilizers for promotion of the interfacial adhesion and properties of immiscible SEBS/TPU blends. *Polym Bull.* <https://doi.org/10.1007/s00289-020-03272-7>
19. Ovejero G, Perez P, Romero MD, Guzman I, Di E (2007) Solubility and Flory Huggins parameters of SBES, poly (styrene-*b*-butene/ethylene-*b*-styrene) triblock copolymer, determined by intrinsic viscosity. *Eur Polym J* 43(4):1444–1449. <https://doi.org/10.1016/j.eurpolymj.2007.01.007>
20. Bragaglia M, Cacciotti I, Cherubini V, Nanni F (2019) Influence of organic modified silica coatings on the tribological properties of elastomeric compounds. *Wear* 434–435:202987. <https://doi.org/10.1016/j.wear.2019.202987>
21. Dackweiler M, Hagemann L, Coutandin S, Fleischer J (2019) Experimental investigation of frictional behavior in a filament winding process for joining fiber-reinforced profiles. *Compos Struct* 229:111436. <https://doi.org/10.1016/j.compstruct.2019.111436>
22. do Amaral FCN, Ernzen JR, Fiorio R, Martins JDN, Dias FTG, Avolio R, Bianchi O, (2018) Effect of the partially hydrolyzed EVA-*h* content on the morphology, rheology and mechanical properties of PA12/EVA blends. *Polym Eng Sci* 58(3):335–344. <https://doi.org/10.1002/pen.24579>
23. Vesna OB, Emi GB, Veljko F (2014) Compatibilization of thermoplastic polyurethane and polypropylene with a SEBS compatibilizer. *Adv Mat Res* 1025–1026:605–614
24. Sengers WGF, Sengupta P, Noordermeer JWM, Picken SJ, Gotsis AD (2004) Linear viscoelastic properties of olefinic thermoplastic elastomer blends: melt state properties. *Polymer* 45(26):8881–8891. <https://doi.org/10.1016/j.polymer.2004.10.030>
25. Sugimoto M, Sakai K, Aoki Y, Taniguchi T, Koyama K, Ueda T (2009) Rheology and morphology change with temperature of SEBS/hydrocarbon oil blends. *J Polym Sci B Polym Phys* 47(10):955–965. <https://doi.org/10.1002/polb.21699>
26. Van Krevelen DW, Te Nijenhuis K (2009) Properties of polymers: their correlation with chemical structure; their numerical estimation and prediction from additive group contributions. Elsevier, Amsterdam
27. Rudolph N, Osswald TA (2014) Polymer rheology: fundamentals and applications. Carl Hanser Verlag GmbH Co KG
28. Bousmina M, Lavoie A, Riedl B (2002) Phase segregation in SAN/PMMA blends probed by rheology, microscopy and inverse gas chromatography techniques. *Macromolecules* 35(16):6274–6283. <https://doi.org/10.1021/ma020053w>
29. Tan L, Su Q, Zhang S, Huang H (2015) Preparing thermoplastic polyurethane/thermoplastic starch with high mechanical and biodegradable properties. *RSC Adv* 5(98):80884–80892. <https://doi.org/10.1039/c5ra09713d>
30. Pavlovsky S, Siegmann A (2009) Chemical sensing materials. I. Electrically conductive SEBS copolymer systems. *J Appl Polym Sci* 113:3322–3329. <https://doi.org/10.1002/app.30310>
31. Sundararaj U, Macosko CW (1995) Drop breakup and coalescence in polymer blends: the effects of concentration and compatibilization. *Macromolecules* 28(8):2647–2657. <https://doi.org/10.1021/ma00112a009>
32. Xiao S, Sue H-J (2019) Effect of molecular weight on scratch and abrasive wear behaviors of thermoplastic polyurethane elastomers. *Polymer* 169:124–130. <https://doi.org/10.1016/j.polymer.2019.02.059>

33. Nunes RW, Martin JR, Johnson JF (1982) Influence of molecular weight and molecular weight distribution on mechanical properties of polymers. *Polym Eng Sci* 22(4):205–228. <https://doi.org/10.1002/pen.760220402>
34. Kim JK, Paglicawan MA, Balasubramanian M (2006) Viscoelastic and gelation studies of SEBS thermoplastic elastomer in different hydrocarbon oils. *Macromol Res* 14(3):365–372. <https://doi.org/10.1007/BF03219096>
35. Thomas S, Kuriakose B, Gupta BR, De SK (1986) Scanning electron microscopy studies on tensile, tear and abrasion failure of plasticized poly (vinyl chloride) and copolyester thermoplastic elastomers. *J Mater Sci* 21(2):711–716. <https://doi.org/10.1007/bf01145545>
36. Hausberger A, Major Z, Theiler G, Gradt T (2018) Observation of the adhesive-and deformation-contribution to the friction and wear behaviour of thermoplastic polyurethanes. *Wear* 412–413:14–22. <https://doi.org/10.1016/j.wear.2018.07.006>
37. Wang C, Hausberger A, Berer M, Pinter G, Grün F, Schwarz T (2019) Fretting Behavior of Thermoplastic Polyurethanes *Lubricants* 7(9):73. <https://doi.org/10.3390/lubricants7090073>

Publisher's Note Springer Nature remains neutral with regard to jurisdictional claims in published maps and institutional affiliations.